Results in Optics 21 (2025) 100890

Contents lists available at ScienceDirect

Results in Optics

journal homepage: www.sciencedirect.com/journal/results-in-optics

Stable and channel spacing tunable of SOA-based multiwavelength fiber laser utilizing parallel Lyot filter

Norasmahan Muridan [a], Abdul Hadi Sulaiman [b,*], Siti Fatimah Norizan [c], Siti Azlida Ibrahim [d,*], Nelidya Md Yusoff [a,*]

[a] Faculty of Artificial Intelligence, Universiti Teknologi Malaysia, Jalan Sultan Yahya Petra, 54100 Kuala Lumpur, Malaysia
[b] School of Physics, Universiti Sains Malaysia, 11800 Gelugor, Penang, Malaysia
[c] IIUM Photonics and Quantum Center, International Islamic University Malaysia, 25200 Kuantan, Pahang, Malaysia
[d] Centre for Fibre Networking and Communication, COE for Intelligent Network, Multimedia University, 63100 Cyberjaya, Selangor, Malaysia

ARTICLE INFO

Keywords:
Multiwavelength fiber laser
Lyot filter
Semiconductor optical amplifier
Intensity dependent loss

ABSTRACT

We proposed the generation of a tunable channel-spacing in a multiwavelength fiber laser that incorporates a semiconductor optical amplifier (SOA) and a parallel Lyot filter. Previously, only a few works demonstrated channel spacing tunability using parallel Lyot filter, with none of them utilizing SOA. A stable and tunable multiwavelength spectrum with up to three distinct channel spacings is demonstrated using three different sets of parallel Lyot filter either Short, Long, and Mixed based on varying lengths of polarization-maintaining fiber (PMF). Channel spacing tunability is achieved by selecting different PMF length combinations. Experimental results show that two channel spacing modes, either single or multiple, can be selected for each configuration. Additionally, increasing the SOA drive current results in a greater number of lasing lines with higher intensity within the cavity. The system demonstrates good stability, with peak power differences of 1.46 dB, 0.65 dB, and 2.61 dB for the Short, Long, and Mixed sets, respectively, during a 60-minute observation period.

1. Introduction

In recent years, multiwavelength fiber lasers (MWFLs) have garnered significant attention because of their diverse applications in optical communication systems, optical sensor, spectroscopy, etc. Unlike single-wavelength lasers, MWFL can emit multiple wavelengths simultaneously, making them particularly suitable for wavelength-division multiplexing systems, which form the foundation of today's high-capacity optical networks. The ability to produce multiple stable and narrow-linewidth wavelengths within a single laser cavity position in MWFL is the key technology in the evolution of advanced optical systems. The growing demand for high-speed, high-capacity data transmission in fiber optic communication has intensified the need to improve the tunability of MWFL. However, achieving tunable channel spacing using a multi-segment Lyot filter based on a semiconductor optical amplifier (SOA) remains a challenge. Despite this, SOAs offer several advantages over erbium-doped fiber amplifier (EDFA) including lower mode competition and broader wavelength bandwidth.

At the core of MWFL design is the wavelength-selective filtering mechanism, which enables the transmission of specific wavelengths. Researchers worldwide have explored various filtering techniques to realize multiwavelength output in fiber lasers. Common approaches include fiber Bragg grating (FBG) (Awang Lah et al., 2023), Mach-Zehnder interferometer (MZI) (Liu et al., 2021), Fabry-Perot filter (Wang et al., 2013), Sagnac loop mirror (SLM) interferometer (Aliza et al., 2025) and Lyot filter (Lah et al., 2024). Each of these methods employs different optical principles for wavelength selection and filtering within the laser cavity, offering distinct benefits and limitations.

Among the various techniques, the Lyot filter has emerged as a highly promising solution for generating multiple lasing wavelengths due to its advantages such as low insertion loss, simple structure, narrow spectral linewidth, high stability and excellent suitability for tunable channel spacing (Chang et al., 2020; Zhou et al., 2020). Traditionally, most Lyot filter-based MWFLs employed EDFA as the gain medium. However, the inherent homogeneous broadening of EDFA leads to strong mode competition, resulting in unstable multiwavelength lasing. To address this, several methods have been proposed, including the

* Corresponding authors.
E-mail addresses: hadisulaiman@usm.my (A.H. Sulaiman), azlida@mmu.edu.my (S.A. Ibrahim), nelidya.kl@utm.my (N.M. Yusoff).

https://doi.org/10.1016/j.rio.2025.100890
Received 15 July 2025; Received in revised form 20 August 2025; Accepted 2 September 2025
Available online 3 September 2025

mechanism of intensity-dependent transmission (IDT) (Sulaiman et al., 2013), intensity-dependent loss (IDL) (Tian et al., 2012) and intracavity four-wave mixing (FWM) (Cholan et al., 2013).

A promising alternative is the use of SOA as the gain medium in Lyot filter-based MWFLs. SOAs exhibit inhomogeneous line expansion, which permits stable multiwavelength spectrum with reduced mode competition and a higher number of lasing lines at room temperature (Sulaiman et al., 2024). Additionally, SOAs do not require an external optical pump, simplifying the setup and eliminating the need for extra components, unlike EDFAs (Sun et al., 2011).

A single segment Lyot filter is typically constructed by inserting a length of polarization-maintaining fiber (PMF) among two polarizers with their axes aligned at 45° to the PMF axes (Sova and Kim, 2002). While several studies have reported Lyot filter-based MWFLs, only a limited number have explored multi-segment Lyot filters with varied configurations (Zhang et al., 2011; Jo et al., 2014). The multiwavelength characteristics can be effectively controlled by adjusting Lyot filter parameters, particularly the PMF length, which directly influences channel spacing. According to the Lyot filter principle, the spacing between wavelength lines can be further controlled by incorporating additional Lyot filter segments within the system (Wang et al., 2012; Li et al., 2017; Chen et al., 2018). Tunable channel spacing can be achieved by manipulating the polarization controller (PC) without changing physical components, while different spacing configurations can be realized by selecting effective PMF lengths (Wei et al., 2021; Zhao et al., 2019; Fok and Shu, 2006). This level of control marks a significant advantage over conventional fiber lasers, which typically offer limited tunability of wavelength spacing. The Lyot filter structure thus provides a flexible platform for precise control over wavelength and interval spacing (Zhang et al., 2012).

Previously, only a few studies on MWFLs using parallel Lyot filters have been reported, primarily employing EDFAs (Qi et al., 2023; Li et al., 2025) and thulium-doped fiber amplifier (TDFA) (Jamalus et al., 2022), with no prior work utilizing SOA. Table 1 presents a comparison of various MWFL works based on the parallel Lyot filter technique, focusing on their tuning ranges and stability. Most reported systems employed EDFA, with one study utilizing a TDFA. In general, parallel Lyot configurations have shown limited tunability, typically under 1 nm. In contrast, our system achieves a significantly broader tuning range of 0.46 nm to 11.6 nm, exceeding all previously reported values and setting a new benchmark for wide channel spacing flexibility. Additionally, our system maintains a stability of 0.65 dB over 60 min, which is competitive with or even better than most EDFA-based systems, although slightly less stable than the narrowest-spacing system reported in Qi et al. (2023). These results highlight the balanced advancement offered by our design, combining exceptional tunability with dependable long-term stability. In this work, we demonstrate a stable MWFL with tunable line spacing utilizing a parallel Lyot filter configuration and SOA as the gain medium. The polarization- and wavelength-dependent cavity transmission enables fine tunability of the multiwavelength output. Three sets of parallel Lyot filters either Short, Long, and Mixed PMF were investigated, each allowing the generation of single or multiple channel spacings. By increasing the SOA drive current, a higher number of lasing lines with enhanced intensity was observed. The stability of the system was validated over a 60-minute period, with peak power differences measured at 0.65 dB, 1.46 dB, and 2.61 dB for the Long, Short, and Mixed sets, respectively.

2. Experimental setup & operating principle

The schematic configuration of the MWFL is illustrated in Fig. 1(a), featuring two segments of Lyot filters as indicated by the blue dotted box. The two blue boxes represent Lyot filter 1 and Lyot filter 2, comprising PC1 which connected to PMF1 and PC2 spliced with PMF2, respectively. A 3 dB coupler (C1) splits the incoming light equally between the two branches, directing 50 % of the light through Lyot Filter 1 and the remaining 50 % through Lyot Filter 2. The outputs from both branches are then recombined using another 3 dB coupler (C2), which feeds the combined signal into a polarizer composed of a PC3 followed by a polarization-dependent isolator (PDI). A polarizer which is from a combination of PC3 and PDI enhances the IDL mechanism, which is essential for achieving a stable and flat multiwavelength spectrum. A linear-type SOA (LSOA) from Thorlabs is employed as the gain medium in the cavity. The laser output is extracted using a 10:90 optical coupler, where 10 % of the output is directed to an optical spectrum analyzer (OSA) with a resolution of 0.02 nm for spectral measurement, while the remaining 90 % is recirculated into the ring cavity to sustain the lasing process through stimulated emission.

Fig. 1(b) illustrates two segments of Lyot filters arranged in parallel namely, Lyot Filter 1 and Lyot Filter 2 which will explain the theoretical foundation of effective length (L_{eff}). The Lyot filters consist of PC1 with PMF1 and PC2 with PMF2. As shown on the left side of the figure, the 3 dB coupler evenly splits the incoming light into both Lyot filter branches. When the light reaches the PC1 and PC2, its transmittance through each branch can be controlled by adjusting the rotation of the PCs with magnitude of E_1 and E_2, respectively. The branch with higher transmittance allows light to pass through and continue in the laser cavity, while the branch with lower transmittance suppresses the light. Therefore, by tuning the PCs, the system can direct the light to propagate through either branch selectively. When only one branch is active within the cavity, the configuration effectively behaves as a single Lyot filter, which can generate a multiwavelength output as described in Zhao et al. (2020). Additionally, the lengths of PMF1 and PMF2 determine the channel spacing of the MWFL. In the parallel Lyot filter configuration, the propagation of light through Lyot Filter 1 and Lyot Filter 2 can be independently controlled by adjusting PC1 and PC2, respectively. Through constructive interference mechanism, when light primarily passes through Lyot Filter 1, the MWFL behaves like a single Lyot filter, and the resulting channel spacing corresponds to the length of PMF1. Similarly, by adjusting the polarization state via PC2, the channel spacing can be made to correspond to the length of PMF2 when light propagates predominantly through Lyot Filter 2.

At specific polarization settings, when both branches permit light transmission simultaneously, the resulting interference produces a channel spacing that corresponds to either the sum or the difference of the PMF1 and PMF2 lengths (L1 and L2), depending on the relative polarization angles (Sova and Kim, 2002; Chen et al., 2018). In essence, the channel spacing in the parallel Lyot filter setup is governed by the L_{eff} which can be defined as either $L1 + L2$ or $|L1 - L2|$, depending on the polarization alignment. As a result, multiple channel spacings can be

Table 1
Performance comparison of several works of MWFL utilizing the parallel Lyot filter technique.

Gain Medium	Type of Comb Filter	Tuning Range (nm)	Peak power deviation (dB)	Duration (min)	Reference
EDFA	Parallel Lyot Filter	0.46–0.88	0.32	30	(Qi et al., 2023)
TDFA	Parallel Lyot Filter	0.9–1.8	–	–	(Jamalus et al., 2022)
EDFA	Cascaded–Parallel Lyot Filter	0.27–0.76	0.78	60	(Yinghui et al., 2025)
EDFA	Parallel Lyot Filter	0.2–0.88	0.64	30	(Lai et al., 2025)
EDFA	Parallel polarization beam splitter	0.46–0.88	0.89	60	(Zhang et al., 2024)
EDFA	Series–Parallel Lyot Filter	0.2–4.36	1.08	30	(Lai et al., 2025)

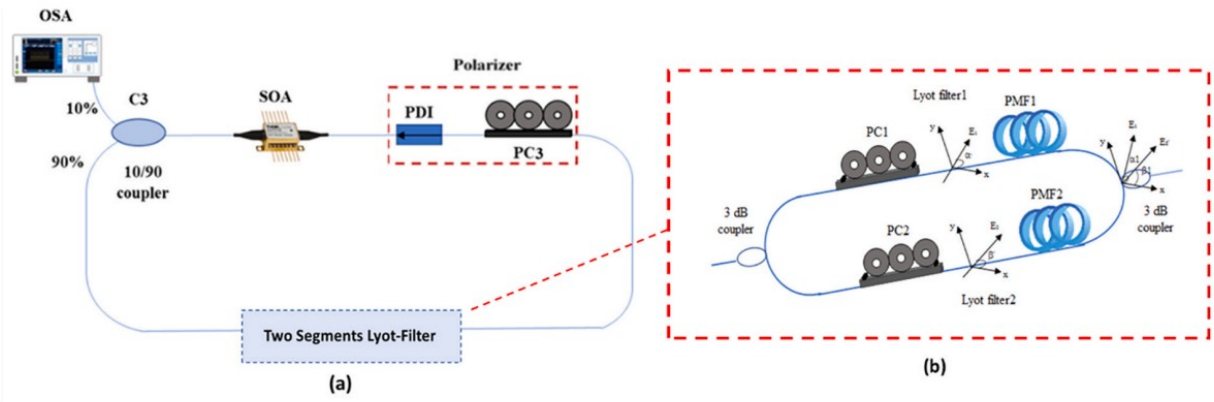

Fig. 1. (a) The experimental structure of MWFL utilizing a parallel Lyot filter incorporating LSOA. (b) The illustration of theoretical foundation of L_{eff} based on two segments of Lyot filters in parallel configuration.

achieved in the proposed MWFL system by manipulating the L_{eff} of the PMF segments within the cavity. The relationship between channel spacing and L_{eff} in a multi-segment Lyot filter system is given by $\Delta\lambda = \lambda^2/BL_{eff}$, where $\Delta\lambda$ is the channel spacing, λ is the operation wavelength and B is the birefringence of the PMF as its value is 3.98×10^{-4}. As demonstrated by Kim and Song (2015), with the increment of temperature, the birefringence value is reduced. Table 2 shows a example of four different of L_{eff} with their calculated L_{eff} and channel spacing. When the polarization axes of the two PMF segments are aligned at 0° angle, the L_{eff} corresponds to the sum of L1 + L2. Conversely, when the polarization axes are orthogonal at 90° angle, the L_{eff} corresponds to the absolute difference of |L1 – L2|.

The IDL mechanism plays a crucial role in enabling stable multiwavelength generation within a laser cavity that employs a homogeneous gain medium. The IDL mechanism arises when the light intensity influences the loss behaviour within the cavity configuration. Specifically, the transmission loss due to IDL mechanism is inversely related to the intracavity light intensity. In ring cavity designs, the IDL effect can be introduced through nonlinear polarization rotation effect, which is typically realized using an SOA in conjunction with polarization control elements like a PC and a polarizer (Lah et al., 2024). Numerous studies have reported the generation of flat multiwavelength spectra by leveraging the IDL mechanism, as demonstrated by (Aliza et al., 2025; Sulaiman et al., 2020). According to previous research, one of the key benefits of incorporating IDL mechanism is its ability to mitigate mode competition, a common issue in homogeneous gain medium such as in EDFA. As a result, the IDL mechanism enables the generation of multiwavelength outputs with narrow channel spacing with high stability (Sulaiman et al., 2018).

3. Results and discussions

The LSOA exhibits amplified spontaneous emission (ASE) at various bias currents, observed at 50 mA intervals, as shown in Fig. 2. It is essential to characterize the ASE before commencing the experiment. At the highest bias current, the highest peak for LSOA is at −31.8 dBm and centered at 1486.9 nm. As the bias current decreases, the peak power gets lower, and the centered wavelength shifts to the longer wavelength.

Table 2
An example of L_{eff} calculation based on two segments Lyot filter for the tunable channel spacing of MWFL.

L_{eff}	Calculated L_{eff} (m)	Channel spacing (nm)
L1	4.41	1.37
L2	2.52	2.27
L1 + L2	6.93	8.72
L1 − L2	1.89	3.20

To investigate the influence of PMF length on channel spacing, three sets of data were examined using different combinations of PMF1 and PMF2 segments. These sets are categorized as Short, Long and Mix, where the lengths of PMF1 and PMF2 are denoted as L1 and L2, respectively. In the Short set, both PMF lengths are less than 1 m, targeting a minimum channel spacing greater than 2 nm. The Long set consists of PMF segments longer than 8 m, while the Mix set combines one PMF from the Short group and the other PMF from the Long group.

Within the MWFL system, where two PMF segments are arranged in parallel as shown in Fig. 1, PC3 is first adjusted to optimize the polarizer's role as an IDL component, ensuring stable multiwavelength generation. Subsequently, PC1 and PC2 are finely tuned to achieve appropriate polarization states that suppress or allow light transmission in each respective branch. Table 3 summarizes the L_{eff} of the PMF segments used in the setup, alongside the experimentally obtained channel spacings ($\Delta\lambda_e$) and the corresponding calculated values ($\Delta\lambda_c$) using Eq. (1).

Based on the experimental results, Fig. 3(a) presents the multiwavelength spectrum obtained from the Short set, exhibiting a wavelength spacing of 11.5 nm, which corresponds to the length of PMF1. The multiwavelength lasing region spans from 1540.4 nm to 1577.0 nm, with the maximum peak power recorded at –14.3 dBm. The extinction ratio (ER) and flatness are measured to be 43.4 dB and 8.4 dB, respectively. Subsequently, PC1 and PC2 are adjusted to suppress the Lyot Filter 1 branch, allowing light to propagate exclusively through the path of Lyot Filter 2. This configuration produces a stable multiwavelength spectrum with five evenly spaced lasing lines, as shown in Fig. 3(b). The channel spacing is 6.2 nm, corresponding to the length of PMF2. The spectrum extends from 1537.6 nm to 1563.8 nm, with the maximum peak power at –17.2 dBm. The measured ER is 41.4 dB and the flatness value is 1.2 dB.

Finally, by carefully tuning PC1 and PC2, both branches are allowed to transmit light simultaneously, resulting in a multiwavelength spectrum with dual channel spacings, as depicted in Fig. 3(c). A magnified display of the spectrum is shown in Fig. 3(d), where two distinct channel spacings of 11.4 nm and 6.4 nm are clearly observed. The lasing spectrum in this configuration ranges from 1520.3 nm to 1568.6 nm, with a maximum peak power of –14.1 dBm and an ER of 40 dB.

For the Long set, when light is directed exclusively through the Lyot Filter 1 branch, a stable multiwavelength output comprising 14 lasing lines is obtained, as shown in Fig. 4(a). The channel spacing is 1.41 nm, corresponding to the length of PMF1. The lasing spectrum spans from 1553.6 nm to 1570.6 nm, with the maximum peak power measured at –16.3 dBm. Next, by adjusting PC1 and PC2 to suppress the Lyot Filter 1 branch, the light is propagated through the Lyot Filter 2 branch. This results in a stable multiwavelength spectrum, as shown in Fig. 4(b), featuring 8 lasing lines with a wavelength spacing of 2.42 nm, which

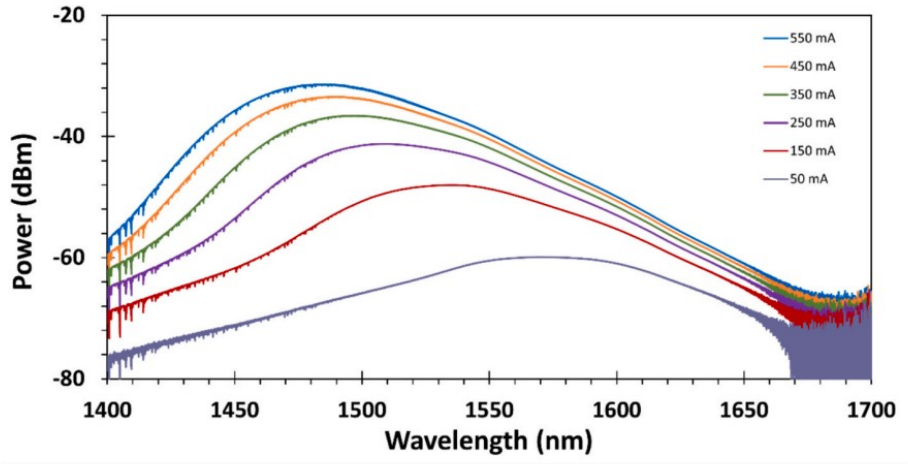

Fig. 2. The ASE of LSOA at different bias current.

Table 3
The PMF length with channel spacing based on experimental work and calculated for single and multiple channel spacing spectra.

Set	PMF Length (m)		Channel spacing calculated, $\Delta\lambda_c$ (nm)	Channel spacing experiment, $\Delta\lambda_e$ (nm)	
				Single spacing spectra	Multiple spacing spectra
Short	**L1**	0.52	11.6	11.5	11.4
	L2	0.98	6.1	6.2	6.4
Long	**L1**	4.41	1.37	1.41	1.46
	L2	2.52	2.27	2.29	2.52
Mix	**L1**	13.20	0.46	0.45	0.47
	L2	2.45	2.45	2.39	2.41

corresponds to the length of PMF2. The spectrum shifts from 1542.3 nm to 1558.6 nm, and the maximum peak power is –14.9 dBm. Both branches are activated by fine-tuning both PC1 and PC2, the resulting lasing spectrum as it exhibits dual channel spacings, as shown in Fig. 4 (c). A magnified view in Fig. 4(d) reveals two distinct channel spacings of 2.52 nm and 1.46 nm. The combined spectrum covers an irregular wavelength range with a bandwidth of approximately 30 nm.

In the Mix set configuration, the lengths of PMF1 and PMF2 are 13.20 m and 0.99 m, respectively. Fig. 5(a) shows the multiwavelength spectrum obtained when PC1 and PC2 are carefully adjusted to allow light to propagate solely through the Lyot Filter 1 branch. Under this condition, the laser achieves multiwavelength operation with 46 lasing lines, exhibiting a line separation of 0.45 nm, which corresponds to the length of PMF1. The maximum peak power is recorded at –19.9 dBm, and the ER is 14 dB.

Subsequently, both PCs are tuned to suppress the Lyot Filter 1 branch, allowing light to pass only through the path of Lyot Filter 2. As shown in Fig. 5(b), the result of a stable spectrum featuring five lasing lines within a 10 dB power range. The observed channel spacing is 6.12 nm, which aligns well with the theoretical value calculated using the formula of wavelength separation. The lasing spectrum spans from 1546.7 nm to 1571.1 nm, with a maximum peak power of –15.9 dBm.

Finally, by carefully fine-tuning PC1 and PC2 to allow simultaneous propagation through both branches, a multiwavelength spectrum with multiple large interference fringes is observed, as illustrated in Fig. 5(c). The large fringe spacing of 5.94 nm is attributed from the length of PMF2. Within these large fringes, finer spectral fringes with a spacing of 0.45 nm, which corresponding to the 13.20 m length of PMF1 are clearly

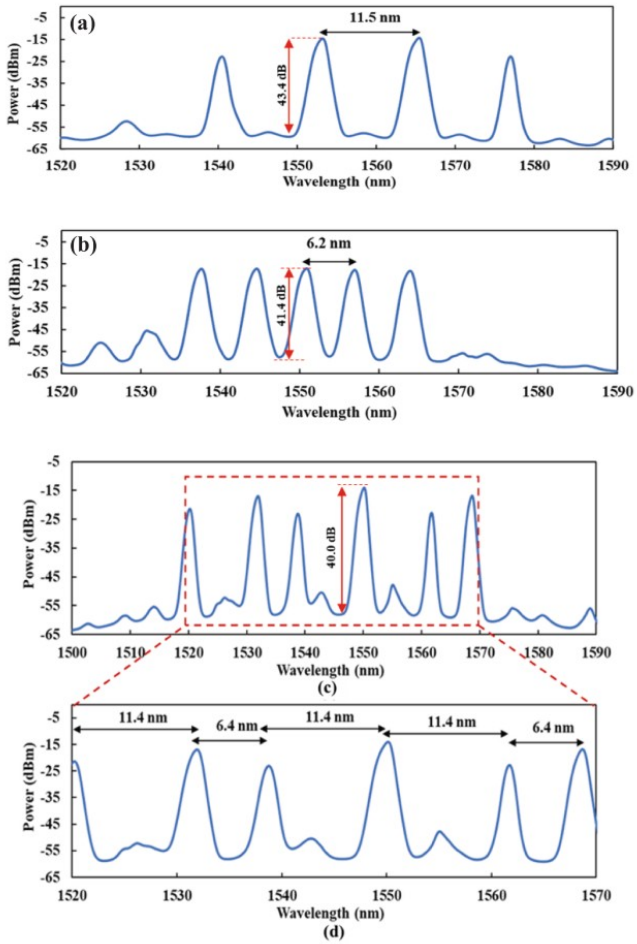

Fig. 3. The multiwavelength spectrum when the L_{eff} is (a) L1, (b) L2, (c) L1 and L2, (d) zoomed in view for the Short set.

visible. The detailed structure of this combined multiwavelength spectrum is further illustrated in the magnified view shown in Fig. 5(d).

Fig. 6(a) presents the multiwavelength spectra of the Short set (L1 and L2) across the 1520–1580 nm of wavelength range, with the SOA currents are varied from 150 mA to 550 mA. It is observed that increasing the SOA current results in a broader spectral bandwidth and a greater channel. At SOA currents of 150 mA, 250 mA, 350 mA, 450 mA,

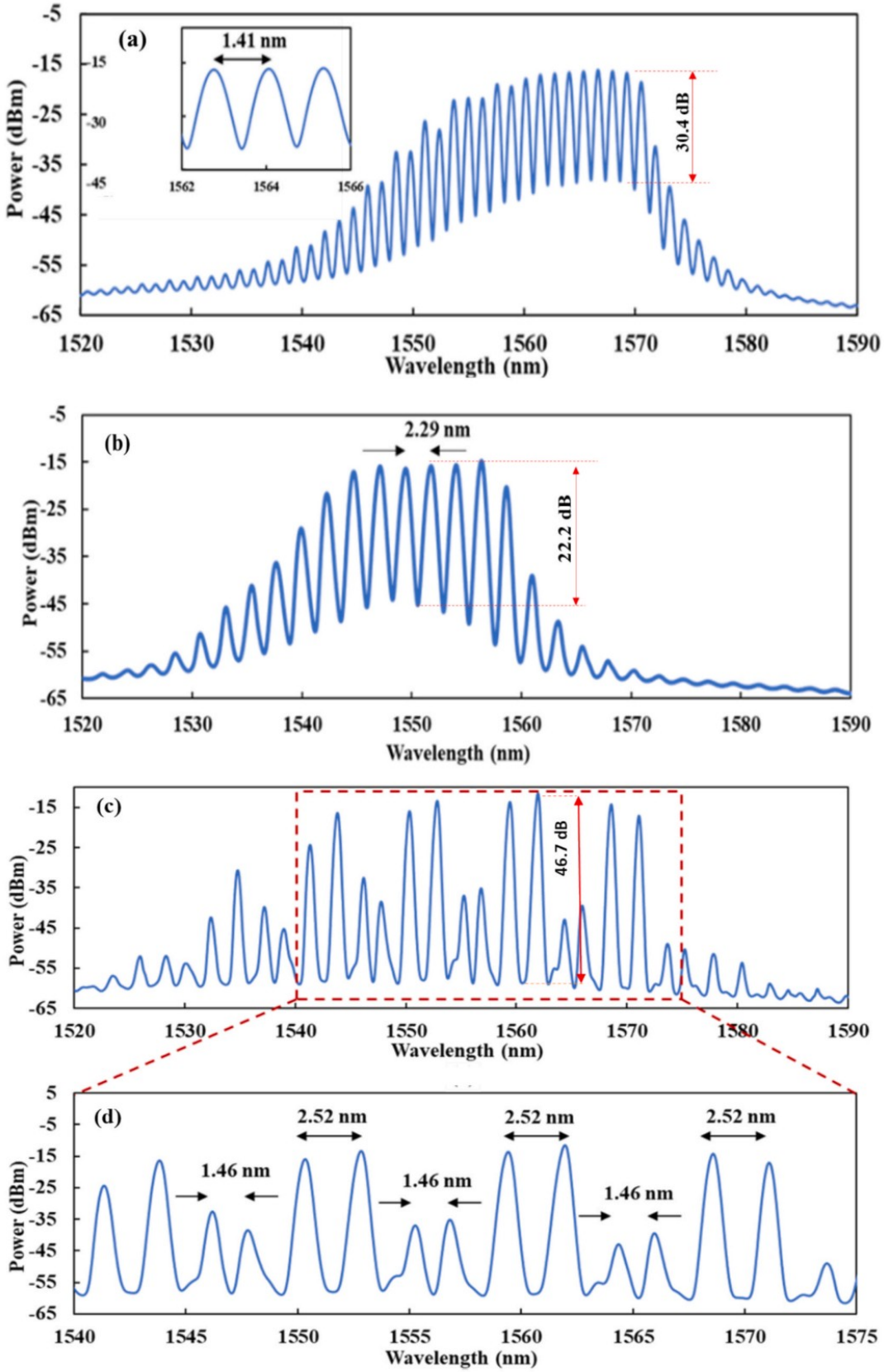

Fig. 4. The multiwavelength spectrum under Long set when the L_{eff} is (a) L1, (b) L2, (c) L1 and L2, (d) magnified view of (c).

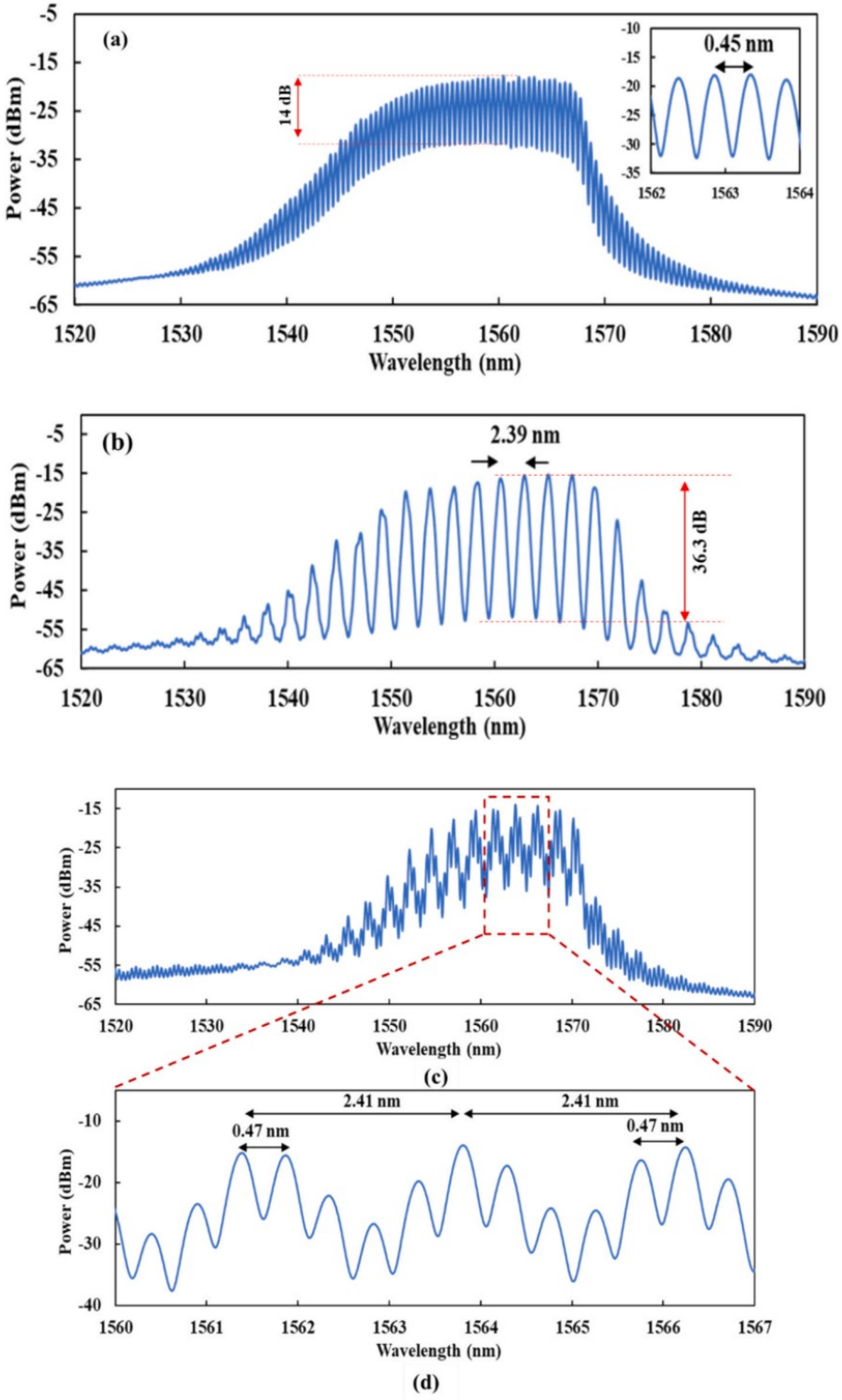

Fig. 5. The multiwavelength spectrum when the L_{eff} is (a) L1, (b) L2, (c) L1 and L2, (d) zoomed in view for L1 and L2 under Mix set.

and 550 mA, the number of channels within a 10 dB bandwidth progressively increases from 2 to 3, 3, 5, and 6, respectively. Correspondingly, the peak power increases from –19.9 dBm to –17.7 dBm, –15.7 dBm, –15.1 dBm, and –14.1 dBm. The measured wavelength bandwidths at each current level are 10.9 nm, 29.5 nm, 29.9 nm, 36.0 nm, and 48.3 nm, respectively. These findings confirm that the intensity inside the ring cavity, which is influenced by the SOA drive current, has a direct impact on both the number of channels and the spectral bandwidth.

Fig. 6(b) shows the multiwavelength spectra for the Long set under the same SOA current range. A similar trend is observed, as the input current increases, the number of lasing lines and the spectral bandwidth both expand. At 150 mA, 4 lasing lines are observed over a 15.7 nm bandwidth. This spectral increases to 7 lasing lines at 250 mA with a 27.3 nm bandwidth. At higher currents of 350 mA, 450 mA, and 550 mA, the number of channels stabilizes at 8, while the bandwidth continues to increase slightly to 27.4 nm, 27.6 nm, and 27.9 nm, respectively. The

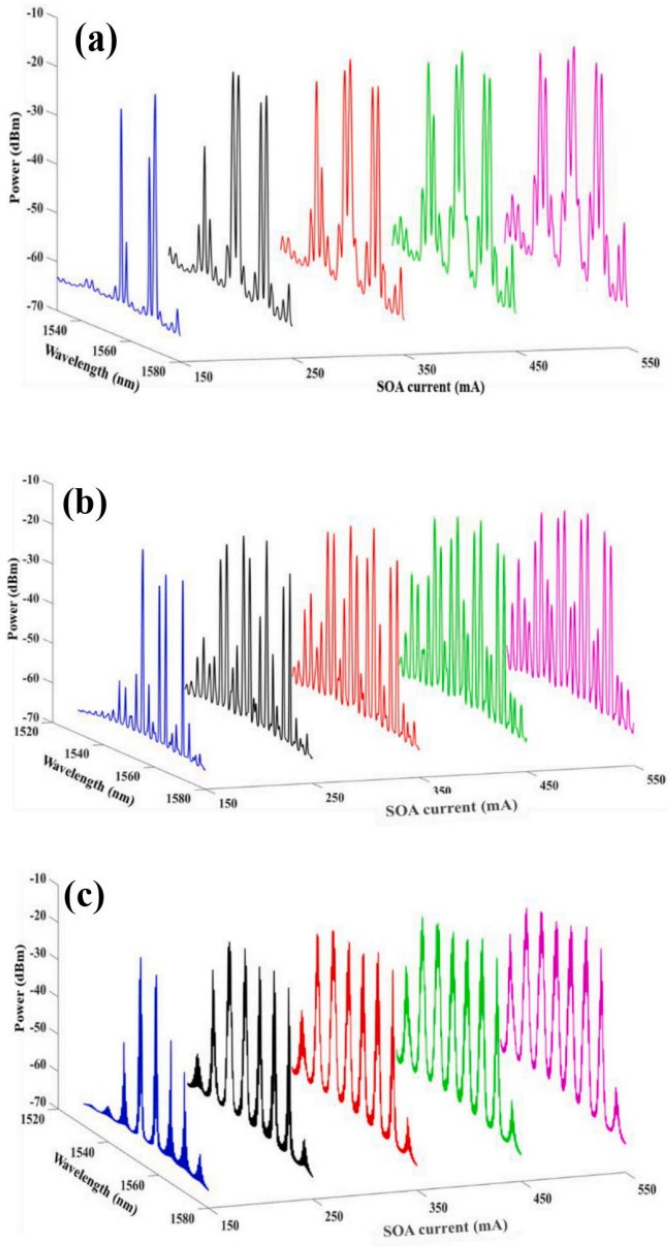

Fig. 6. The multiwavelength spectra at increased SOA current for L1 and L2 under (a) Short set, (b) Long set and (c) Mix set.

corresponding peak power rises from –16.5 dBm at 150 mA to –14.1 dBm, –14.0 dBm, –13.9 dBm, and –13.8 dBm as the SOA current increases. The results validate that both spectral bandwidth and peak power improved with higher SOA current. Additionally, the channel spacing intervals remain consistent across all SOA current levels, although slight shifts in the central wavelength are observed.

Fig. 6(c) illustrates the spectral behaviour for the Mix set under varying SOA currents. Small spectral fringes are apparent in the output, and the number of channels increases with higher input current. At 150 mA and 250 mA, 5 lasing lines are observed within a 10 dB power range. As the current increases further, the number of lines grows accordingly. The peak power improves from –16.5 dBm to –14.1 dBm, –14.0 dBm, –13.9 dBm, and –13.8 dBm for SOA currents of 150 mA, 250 mA, 350 mA, 450 mA, and 550 mA, respectively. The wavelength bandwidth also increases, measured at 6.9 nm, 9.7 nm, 13.6 nm, 15.8 nm, and 16.0 nm for the respective current levels. These findings confirm that increased SOA current enhances both peak power and spectral bandwidth, reaffirming the influence of cavity intensity on the lasing performance.

Table 4 presents a summary of key spectral characteristics including the number of lasing lines, wavelength range, spectral bandwidth, peak power, and ER for the Short, Long, and Mix sets under varying SOA bias currents. All spectra correspond to the multiple spacing configurations, where both PMF1 and PMF2 (L1 and L2) are active. As the SOA current increases from 150 mA to 550 mA in steps of 100 mA, a clear increase in the number of channels is observed across all sets. The expansion in wavelength range between the lowest and highest current levels is 13.5 nm for the Short set, 11.6 nm for the Long set, and 24.0 nm for the Mix set. These results indicate that higher SOA current contributes to broader spectral generation.

Additionally, with increasing bias current, the spectra exhibit a noticeable shift of the center wavelength toward shorter wavelengths in all three sets. This shift is accompanied by an increase in peak power, attributed to the enhanced IDL mechanism at higher SOA currents. Regarding ER, both the Short and Long sets show improvements of 6.0 dB and 4.6 dB, respectively, as the SOA current increases from 150 mA to 550 mA. In contrast, the Mix set exhibits the most noticeable flatness compared to the Short and Long sets. This flatness corresponds to a reduction in ER at higher intensities, which is a trade-off for achieving a greater number of lasing lines. In other words, increasing the SOA current broadens the gain bandwidth and raises the intracavity intensity, thereby increasing the number of channels. However, this also leads to a reduction in ER.

To evaluate the stability of the output, the spectra with multiple channel spacings were recorded at 6-minute intervals over a 60-minute period. Fig. 7(a) presents 11 recorded spectra for the Short set, covering the wavelength range from 1530 nm to 1590 nm. The results indicate excellent wavelength stability and consistent peak power over time. For a more detailed analysis, Fig. 7(b) highlights the temporal variation of peak power of three selected laser wavelengths: 1540 nm, 1552 nm, and 1567 nm. At 1540 nm, the peak power fluctuates between a maximum of –14.8 dBm and a minimum of –16.03 dBm, resulting in a total variation of 1.23 dB. The highest difference of 0.37 dB occurs between the 54th and 60th minute, while the smallest difference of 0.02 dB is observed between the 42nd and 48th minute.

The MWFL exhibits good spectral and power stability during continuous operation, as detailed in the following discussion. The maximum power difference is 1.46 dB, while the minimum is 0.16 dB. Initially, the lasing stability was monitored at a wavelength of 1552 nm, with a maximum power fluctuation of 2.66 dB. The largest difference of 1.41 dB occurred between the 0th and 6th minute, while the smallest difference of 0.03 dB was recorded between the 18th and 24th minute. The primary cause of high peak power fluctuations originates from the PMF that is not maintained under isothermal conditions. Therefore, stabilizing the PMF by cooling it in a thermostatic ice bath at a constant temperature can enhance the laser's stability as demonstrated in Zhao et al. (2018). At a wavelength of 1567 nm, the maximum and minimum peak powers were –14.88 dBm and –17.6 dBm, respectively, resulting in a total variation of 2.72 dB.

Fig. 8(a) presents 11 recorded spectra for the Long set over a 10 nm wavelength span from 1550 nm to 1580 nm. The overall spectral profile demonstrates minor fluctuations throughout the 60-minute observation period. To analyze peak power stability in more detail, three lasing wavelengths; 1558 nm, 1565 nm, and 1568 nm were selected, with their variations shown in Fig. 8(b). At 1558 nm, the peak power ranges from a maximum of –15.05 dBm to a minimum of –16.4 dBm, resulting in a fluctuation of 1.35 dB. The largest difference, 0.77 dB, occurs between the 36th and 42nd minute, while the smallest difference, 0.07 dB, is recorded between the 6th and 12th minute.

For the 1565 nm wavelength, the peak power varies from –16.0 dBm to –19.09 dBm, yielding a total fluctuation of 3.09 dB. The highest difference of 2.00 dB is observed between the 36th and 42nd minute, and the lowest difference of 0.04 dB occurs between the 12th and 18th minute. At 1568 nm, the difference between the highest and the lowest

Table 4
The number of lasing lines, wavelength range, wavelength bandwidth, peak power and ER at different SOA current of (L1 and L2) for Short (S), Long (L) and Mix (M) spectra.

SOA current (mA)	Parameter											
	Number of lasing lines			Wavelength range (nm) / Multiwavelength bandwidth (nm)			Highest peak power (dBm)			ER (dB)		
	S	L	M	S	L	M	S	L	M	S	L	M
150	2	4	5	1550.9–1561.8/10.9	1555.4–1571.2/15.7	1568.6–1575.5/6.9	−19.9	−16.3	−16.5	27.7	42.1	43.1
250	3	7	5	1532.6–1562.1/29.5	1543.9–1571.2/27.3	1561.4–1571.1/9.7	−17.7	−13.8	−14.1	28.8	44.5	41.2
350	3	8	7	1532.4–1562.3/29.9	1543.8–1571.2/27.4	1557.1–1570.7/13.6	−15.7	−12.1	−14.0	31.1	46.2	40.8
450	5	8	8	1532.2–1568.2/36.0	1543.9–1571.5/27.6	1554.8–1570.6/15.8	−15.1	−11.7	−13.9	31.9	46.6	26.2
550	6	8	8	1520.3–1568.6/48.3	1541.2–1569.1/27.9	1554.6–1570.6/16.0	−14.1	−11.6	−13.8	33.7	46.7	22.1

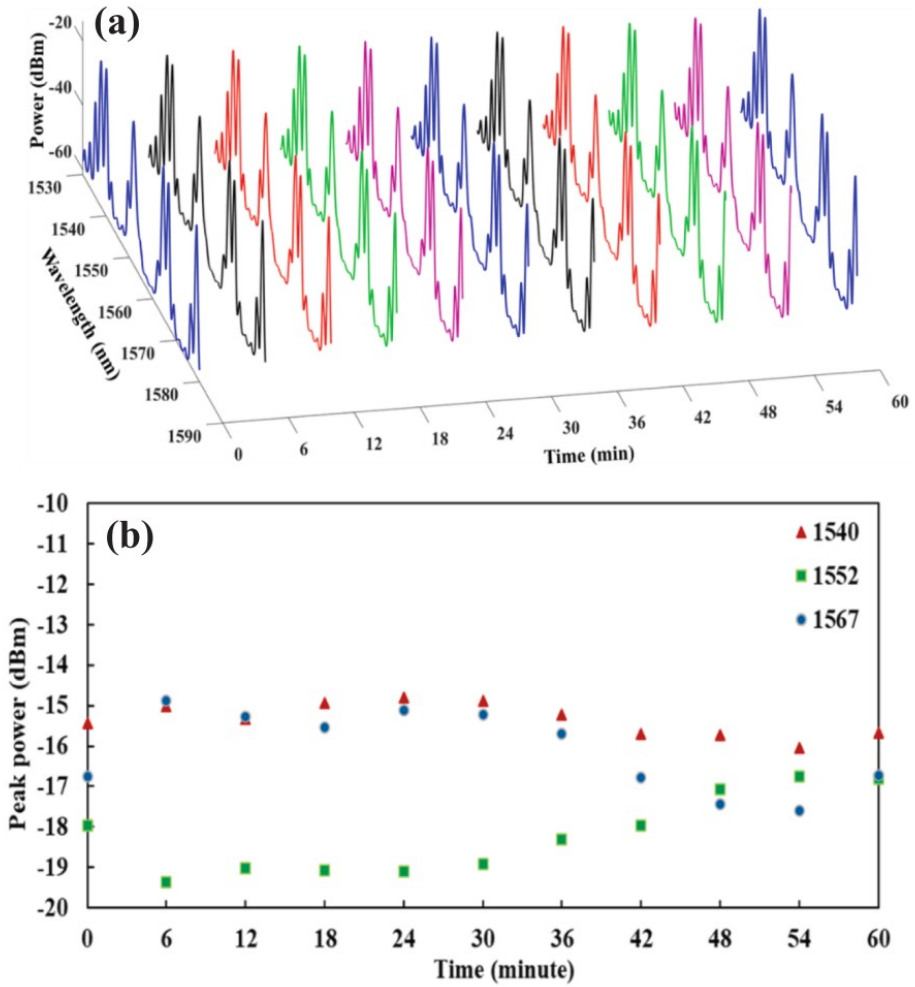

Fig. 7. (a). The stability observation of the LSOA and (b) the observation of peak power differences of three laser wavelengths within 1 hour for L1 and L2 of the Short set.

peak power is 1.05 dB. The highest difference recorded is 0.65 dB from the 36th to 42nd minute, while the minimum is 0.08 dB from the 0th to 6th minute. These results confirm that the Long set exhibits good spectral stability, with only slight variations in peak power over time.

Fig. 9(a) displays 11 recorded spectra over a 10 nm from 1550 nm to 1580 nm for the Mix set. To assess the peak power stability, three lasing wavelengths; 1562 nm, 1567 nm, and 1568 nm were selected for detailed analysis, as shown in Fig. 9(b). At 1562 nm, the peak power varies between a maximum of –15.06 dBm and a minimum of –17.55 dBm, resulting in a total fluctuation of 1.87 dB. The highest difference of 1.87 dB happens during the 0th to 6th minute, while the lowest difference, 0.1 dB, is recorded between the 24th and 30th minute.

For the wavelength at 1567 nm, the peak power ranges from –15.07 dBm to –16.53 dBm, corresponding to a variation of 1.46 dB. The maximum difference of 1.31 dB is observed from the 0th to 6th minute, whereas the minimum difference of 0.01 dB occurs between the 36th and 42nd minute. At 1568 nm, a peak power difference of 3.34 dB is recorded, with the highest and lowest values being –14.94 dBm and –18.28 dBm, respectively. The greatest difference, 2.61 dB, occurs between the 48th and 54th minute, while the smallest difference of 0.01 dB is observed from the 36th to 42nd minute. These findings indicate that while the Mix set exhibits generally stable lasing behaviour, certain wavelengths may experience higher peak power fluctuations, especially during specific time intervals.

In the prior art, especially MWFL based on Lyot filter, the lowest peak power deviation of 0.25 dB is exhibited by 1590 nm, demonstrated by

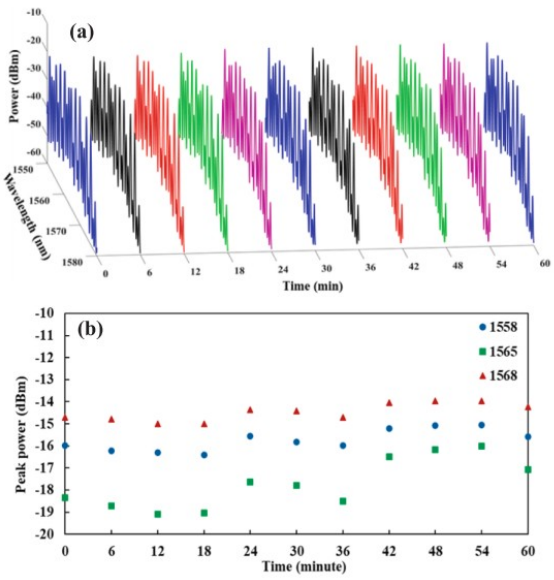

Fig. 8. (a). The stability observation of the LSOA and (b) the observation of peak power differences of three lasing wavelengths within 1 hour for L1 and L2 of the Long set.

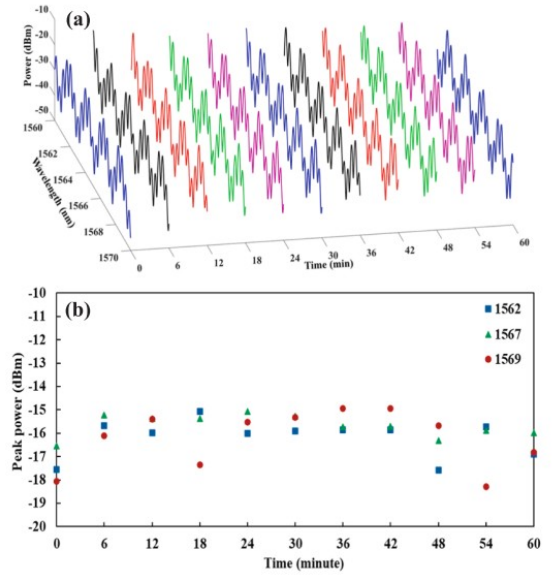

Fig. 9. (a). The stability observation of the LSOA and (b) the observation of peak power variations of three lasing wavelengths within 60 min for L1 and L2 of the Mix set.

Lah et al. (2024). Muridan et al. has peak power deviation of 0.17 dB at 1631 nm (Muridan et al., 2021). Meanwhile, the lowest laser fluctuation is 1.01 dB at the lasing wavelength of 1564.8 nm as in Reference (Sulaiman et al., 2018). Ultimately, the application of MWFL is used in spectroscopy as tunable light sources for spectroscopic analysis, particularly in environments that demand narrow linewidths and high output stability. It is also applied in optical sensing and fiber sensor arrays, supporting measurements in temperature, strain, gas detection, and structural health monitoring.

4. Conclusions

This paper has presented an experimental study on the generation of MWFL using a parallel configuration of two-segment of Lyot filters based on SOA. The system comprises Lyot Filter 1 and Lyot Filter 2, consisting of PC1 with PMF1 and PC2 with PMF2, respectively. The results demonstrated that fine adjustments of the PCs significantly influence the L_{eff} of the PMFs, thereby affecting the spectral output. By tuning the PCs, the transmission characteristics of the light through each Lyot filter's branch can be precisely controlled. The investigation was conducted using three configurations of PMF length, referred to as the Short, Long, and Mix sets which correspond to PMF lengths of L1, L2 and the combination of L1 and L2, respectively. Each configuration produced multiwavelength spectra with distinct characteristics in terms of wavelength range, spectral bandwidth, peak power and ER. With increasing SOA drive current, all three sets exhibited a consistent trend of increased lasing lines, attributed from the enhanced intracavity intensity provided by the SOA. In terms of stability, the maximum peak power differences recorded over a 60-minute observation period were 1.46 dB for the Short set, 0.65 dB for the Long set, and 2.61 dB for the Mix set, confirming reliable and stable performance of the proposed MWFL system.

CRediT authorship contribution statement

Norasmahan Muridan: Writing – review & editing, Writing – original draft, Data curation. **Abdul Hadi Sulaiman:** Writing – review & editing, Supervision, Conceptualization. **Siti Fatimah Norizan:** Writing – review & editing. **Siti Azlida Ibrahim:** Funding acquisition. **Nelidya Md Yusoff:** Validation, Supervision, Project administration, Funding acquisition.

Declaration of competing interest

The authors declare the following financial interests/personal relationships which may be considered as potential competing interests: Nelidya Md Yusoff reports financial support was provided by Universiti Teknologi Malaysia. Abdul Hadi Sulaiman reports a relationship with Universiti Tenaga Nasional that includes: employment. If there are other authors, they declare that they have no known competing financial interests or personal relationships that could have appeared to influence the work reported in this paper.

Acknowledgements

This research was partly financially supported by Universiti Teknologi Malaysia under the UTM Fundamental Research (Q. K130000.3856.22H95). This work was also supported by Tenaga Nasional Berhad (TNB) and Universiti Tenaga Nasional (UNITEN) through the BOLD Refresh Postdoctoral Fellowships under the project code of J510050002-IC-6 BOLDREFRESH2025-Centre of Excellence.

Declaration

During the preparation of this work the author(s) used ChatGPT to improve the English language of several sentences. After using this tool/service, the author(s) reviewed and edited the content as needed and take(s) full responsibility for the content of the publication.

Data availability

Data will be made available on request.

References

Aliza, H.E.M., Sulaiman, A.H., Ismail, A., Abdullah, F., Yusoff, N.M., Ibrahim, S.A., et al., 2025. Enhanced multiwavelength random fiber laser based on hybrid optical amplifier incorporating Sagnac loop mirror interferometer. Results Phys. 72, 1–10. https://doi.org/10.1016/j.rinp.2025.108212.

Awang Lah, A.A., Sulaiman, A.H., Abdullah, F., Ambran, S., Ng, E.K., Alresheedi, M.T., et al., 2023. Stable triple-wavelength random fiber laser based on fiber Bragg gratings. Photonics 10, 1–10. https://doi.org/10.3390/photonics10080924.

Chang, Y., Pei, L., Ning, T., Zheng, J., Li, J., Xie, C., 2020. Switchable and tunable multi-wavelength fiber ring laser employing a cascaded fiber filter. Opt. Fiber Technol. 58. https://doi.org/10.1016/j.yofte.2020.102240.

Chen, J., Tong, Z., Zhang, W., Xue, L., Pan, H., 2018. Research on tunable multiwavelength fiber lasers with two-section birefringence fibers and a nonlinear optical loop. Laser Phys. 28. https://doi.org/10.1088/1555-6611/aab24e.

Cholan, N.A., Al-Mansoori, M.H., Noor, A.S.M., Ismail, A., Mahdi, M.A., 2013. Multi-wavelength generation by self-seeded four-wave mixing. Opt. Express 21, 6131. https://doi.org/10.1364/oe.21.006131.

Fok, M., Shu, C., 2006. A cascadable approach to produce widely selectable spectral spacing in birefringent comb filters. IEEE Photon. Technol. Lett. 18, 1937–1939.

Jamalus, M.S.K., Sulaiman, A.H., Abdullah, F., Zulkifli, N., Alresheedi, M.T., Mahdi, M. A., et al., 2022. Selectable multiwavelength thulium-doped fiber laser based on parallel Lyot filter. Opt. Fiber Technol. 70, 102892. https://doi.org/10.1016/j.yofte.2022.102892.

Jo, S., Park, K., Lee, Y.W., 2014. Lyot-type flat-top fibre multiwavelength filter based on polarisation-diversity loop structure. Micro Nano Lett. 9, 858–861. https://doi.org/10.1049/mnl.2014.0386.

Kim, Y.H., Song, K.Y., 2015. Characterization of temperature-dependent birefringence in polarization maintaining fibers based on Brillouin dynamic gratings. Fifth Asia-Pac. Opt. Sens. Conf. 9655, 96553N. https://doi.org/10.1117/12.2185008.

Lah, A.A.A., Sulaiman, A.H., Abdullah, F., Yusoff, N.M., 2024. Multiwavelength fiber laser based on enhanced bidirectional SOA utilizing Lyot filter. Optik (Stuttg) 301, 171679. https://doi.org/10.1016/j.ijleo.2024.171679.

Lai, M., Zhou, X., Lu, Y., Hu, M., 2025. Design and analysis of an improved parallel Lyot filter based on secondary interference. Opt. Eng. 64, 1–15. https://doi.org/10.1117/1.oe.64.4.046101.

Lai, M., Zhou, X., Xia, Y., Hu, M., 2025. Laser-oriented design and performance analysis of series-parallel lyot filters with cross-output. Opt. Fiber Technol. 94, 104363. https://doi.org/10.1016/j.yofte.2025.104363.

Li, Y., Tian, J., Quan, M., Yao, Y., 2017. Tunable multiwavelength fiber laser with a two-stage Lyot filter. IEEE Photon. Technol. Lett. 29, 287–290. https://doi.org/10.1109/LPT.2016.2644672.

Li, Y., Pan, H., You, Q., Li, B., Zhu, Y., Li, R., et al., 2025. Switchable and wavelength-spaced tunable multi-wavelength actively Q-switched fiber laser based on EOM and parallel Lyot filters. Opt. Fiber Technol. 90. https://doi.org/10.1016/j.yofte.2025.104138.

Liu, J., Tong, Z., Zhang, W., Shi, X., Li, J., 2021. Tunable multi – wavelength random distributed feedback fiber laser based on dual – pass MZI. Appl. Phys. B 127, 1–9.

Muridan, N., Sulaiman, A.H., Abdullah, F., Yusoff, N.M., 2021. Effect of polarization adjustment towards the performance of SOA-based multiwavelength fiber laser. Optik (Stuttg) 242, 167007. https://doi.org/10.1016/j.ijleo.2021.167007.

Qi, H., Zhou, X., Bi, M., Yang, G., Hu, M., Li, H., 2023. Switchable and tunable multi-wavelength random distributed feedback fiber laser based on parallel Lyot filter. Opt. Fiber Technol. 81, 103519. https://doi.org/10.1016/j.yofte.2023.103519.

Sova, R., Kim, C., 2002. Tunable dual-wavelength all-PM fiber ring laser. IEEE Photon. Technol. Lett. 14, 287–289.

Sulaiman, A.H., Zamzuri, A.K., Hitam, S., Abas, A.F., Mahdi, M.A., 2013. Flatness investigation of multiwavelength SOA fiber laser based on intensity-dependent transmission mechanism. Opt. Commun. 291, 264–268. https://doi.org/10.1016/j.optcom.2012.10.078.

Sulaiman, A.H., Yusoff, N.M., Cholan, N.A., Mahdi, M.A., 2018. Multiwavelength fiber laser based on bidirectional Lyot filter in conjunction with intensity dependent loss mechanism. Indonesian J. Electr. Eng. Comput. Sci. 10, 401–408. https://doi.org/10.11591/ijeecs.v10.i3.ppab-cd.

Sulaiman, A.H., Zamzuri, A.K., Md Yusoff, N., Cholan, N.A., Abdullah, F., Abas, A.F., et al., 2018. Broad bandwidth SOA-based multiwavelength laser incorporating a bidirectional Lyot filter. Chin. Opt. Lett. 16, 1–6. https://doi.org/10.3788/COL201816.090603.1.

Sulaiman, A.H., Yusoff, N.M, Abdullah, F., Mahdi, M.A., 2020. Tunable multiwavelength fiber laser based on bidirectional SOA in conjunction with Sagnac loop mirror interferometer. Results Phys. 18, 1–5. https://doi.org/10.1016/j.rinp.2020.103301.

Sulaiman, A.H., David, A.P., Ismail, A., Abu Hassan, N.N., Abdullah, F., Jamaludin, M.Z., et al., 2024. Sagnac-interferometer-based multiwavelength SOA fiber laser assisted by an intensity-dependent loss mechanism. Appl. Opt. 63, 1241–1246. https://doi.org/10.1364/ao.506145.

Sun, G., Zhou, Y., Hu, Y., Chung, Y., 2011. Polarization controlled tunable multiwavelength SOA-fiber laser based on few-mode polarization maintaining fiber loop mirror. Opt. Fiber Technol. 17, 79–83. https://doi.org/10.1016/j.yofte.2010.10.009.

Tian, J., Yao, Y., Xiao, J.J., Yu, X., Chen, D., 2012. Tunable multiwavelength erbium-doped fiber laser based on intensity-dependent loss and intra-cavity loss modulation. Opt. Commun. 285, 2426–2429. https://doi.org/10.1016/j.optcom.2012.01.034.

Wang, W., Meng, H., Wu, X., Xue, H., Tan, C., Huang, X., 2012. Three channel-spacing switchable multiwavelength fiber laser with two segments of polarization-maintaining fiber. IEEE Photon. Technol. Lett. 24, 470–472.

Wang, Y., Xia, L., Yang, C., Zhang, Y., Li, L., Xie, Z., et al., 2013. Multiwavelength generation based on a mode-locked fiber laser using carbon nanotube and fiber Fabry-Perot filter. Appl. Opt. 52, 6616–6619.

Wei, L., Xu, X., Khattak, A., Henley, B., 2021. Continuously tunable comb filter based on a high-birefringence fiber loop mirror with a polarization controller. J. Lightwave Technol. 39, 4800–4808. https://doi.org/10.1109/JLT.2021.3077252.

Yinghui, Z., Xuefang, Z., Minquan, L., 2025. A wavelength interval switchable erbium-doped fiber laser based on cascaded and parallel Lyot filters. Optoelectron. Lett. 21, 0257–0264.

Zhang, Z., Liang, P., Sang, M., Zhiqing, Y., 2011. Wavelength-spacing switchable multiwavelength fiber lasers based on nonlinear polarization rotation with cascaded birefringence fibers. J. Mod. Opt. 58, 82–86. https://doi.org/10.1080/09500340.2010.536591.

Zhang, Z., Zhang, L., Xu, Z., 2012. Tunable multiwavelength ytterbium-doped fiber laser based on nonlinear polarization rotation. J. Nonlinear Opt. Phys. Mater. 21, 1–7. https://doi.org/10.1142/S0218863512500415.

Zhang, Y., Zhou, X., Lai, M., Hu, M., 2024. Design and analysis of parallel polarization-beam-splitter-based optical filter with adjustable channel spacing. Opt. Rev. 31, 664–673. https://doi.org/10.1007/s10043-024-00920-5.

Zhao, Z., Li, X., Li, Y., Qin, H., Wang, H., Luo, Y., et al., 2018. Multiwavelength Er-doped fiber laser using an all-fiber Lyot filter. Appl. Opt. 57, 9270. https://doi.org/10.1364/ao.57.009270.

Zhao, Q., Pei, L., Zheng, J., Tang, M., Xie, Y., Li, J., et al., 2019. Switchable multi-wavelength erbium-doped fiber laser with adjustable wavelength interval. J. Lightwave Technol. 37, 3784–3790. https://doi.org/10.1109/jlt.2019.2920840.

Zhao, Q., Pei, L., Zheng, J., Tang, M., Xie, Y., Li, J., et al., 2020. Tunable and interval-adjustable multi-wavelength erbium-doped fiber laser based on cascaded filters with the assistance of NPR. Opt. Laser Technol. 131, 106387. https://doi.org/10.1016/j.optlastec.2020.106387.

Zhou, X., Hao, H., Bi, M., Yang, G., Hu, M., 2020. Multi-wavelength SOA fiber laser with ultra-narrow wavelength spacing based on multi-wavelength SOA fiber laser with ultra-narrow wavelength spacing based on NPR effect (1–9). IEEE Photonics J. 12, 7202408. https://doi.org/10.1109/JPHOT.2020.3024104.